

Method for measuring the Raman gain tensor in optical fibers

Idan Mandelbaum

Physics Laboratory, National Institute of Standards and Technology, Gaithersburg, Maryland 20899

Maxim Bolshtyansky

JDS Uniphase Corporation, West Trenton, New Jersey 08638

Tony F. Heinz

Departments of Physics and Electrical Engineering, Columbia University, New York, New York 10514

Angela R. Hight Walker

Physics Laboratory, National Institute of Standards and Technology, Gaithersburg, Maryland 20899

Received June 3, 2005; revised October 5, 2005; accepted October 11, 2005; posted October 14, 2005 (Doc. ID 62560)

We present a technique to measure the tensor components of the Raman gain spectrum in a short piece of optical fiber. Using this approach, we obtain results for the frequency dependence of the Raman gain tensor in a silica-based fiber for Raman shifts from less than 1 to over 15 THz. We compare these data with measurements of spontaneous Raman scattering in bulk silica and find good agreement for the depolarization ratio, including in the low-frequency regime. © 2006 Optical Society of America
OCIS codes: 060.2300, 190.5650, 190.4370.

1. INTRODUCTION

The Raman response of silica glasses including the behavior for small frequency shifts, is of both fundamental and practical importance. From the fundamental side, interest has focused on the utility of the Raman response for probing the structural properties of the material.^{1,2} From the point of applications, the significance of the Raman response lies in the Raman gain phenomenon that couples light waves at differing frequencies in an optical fiber. This process is essential for recent advances in wideband optical amplification but can also adversely affect the performance of dense wavelength-division-multiplexed systems through the channel-channel interactions that it induces.³

The Raman response of silica previously has been characterized by using measurements of spontaneous Raman scattering^{1,2,4} and of the Raman gain (or stimulated Raman) process.⁵⁻⁷ In both of these types of measurement, it has been possible to access the spectral characteristics of Raman interaction, as well as its tensor properties, through control of the light polarization. There is broad agreement between the results of the spontaneous Raman experiments, typically performed by using bulk samples of glass, and the stimulated Raman measurements, typically performed in optical fibers. Recent Raman gain studies in silica-based optical fiber^{5,6} have, however, implied tensor properties of the Raman response for small frequency shifts that deviate from the results of the spontaneous Raman measurements. Specifically, the depolarization ratio, defined as the ratio of the perpendicular-to-

parallel Raman gain coefficients, was found to be higher in the Raman gain measurements than in the earlier spontaneous Raman measurements for frequency shifts below 1 THz. This discrepancy was noted by Dougherty and co-workers⁵ and by Stolen.⁷ Factors that might contribute to this discrepancy include differences in the stoichiometry and processing of the materials (bulk glass samples versus optical fibers), as well as different choices of the Raman pump wavelengths (visible wavelengths versus near-infrared wavelengths).

In this paper we present an experimental approach specifically designed to measure the tensor properties of the Raman gain in optical fibers over a wide range of Raman frequency shifts, including the regime of small frequency shifts. In the method, we directly determine the frequency-dependent Raman gain experienced by a variable-wavelength probe pulse propagating through an optical fiber in the presence of a monochromatic Raman pump beam. The tensor properties of the Raman interaction are determined by appropriate control of the relative pump and probe polarizations. A key aspect of the method is the use of a phase-sensitive double-modulation technique. This approach permits ready separation of the Raman gain of the probe beam from the Rayleigh background produced by elastic scattering of the strong pump beam. The isolation mechanism, it should be noted, does not require specialized optical filtering, which may otherwise limit the choice of frequencies of the measurements. In addition, the double-modulation scheme eliminates, to first order, the influence of any frequency-dependent lin-

ear loss in the fiber on the measurement. These features render the approach a reliable and sensitive measurement technique that permits characterization of segments of fiber as short as a few meters. The method is also appropriate for probing the difficult regime of small Raman frequency shifts.

In addition to describing the experimental methodology and the underlying theory of the measurement in this paper, we also report data on the polarized Raman gain for a silica-based optical fiber for Raman shifts ranging from less than 1 to above 15 THz for a Raman pump beam at 1460 nm. These data yield the frequency-dependent Raman depolarization ratio, which we find to be $D = 0.30 \pm 0.05$ for frequencies below 1 THz. To understand the origin of discrepancy previously observed in this quantity, we have also performed polarized spontaneous Raman-scattering measurements from bulk fused-silica samples. Although both the detailed composition of the samples and the Raman pump frequencies differed, we obtained excellent agreement between the two measurements. This agreement demonstrates the accuracy of the fiber-based measurement, even for small Raman shifts, and indicates its suitability for characterizing a variety of optical fibers of importance for applications.

2. THEORY

We first present the theoretical background necessary for the interpretation of our experimental determination of the tensor Raman gain coefficients.

A. Analysis of Raman Gain for Parallel and Perpendicular Pump and Probe Polarization States

The measurements are carried in a polarization-maintaining single-mode optical fiber. The Raman gain is induced by a strong monochromatic pump beam at (angular) frequency ω_p . The Raman gain is measured by a weak probe beam at a lower frequency ω_s , corresponding to a Raman frequency shift of $\omega_p - \omega_s$. To simplify separation of the Raman pump beam and the probe beam in the experiment, we adopt a counterpropagating geometry in which the probe beam travels through the fiber of length L from position from $z=0$ to $z=L$ while the pump beam travels from $z=L$ to $z=0$. Neglecting pump depletion and spontaneous emission, we can then describe the probe power as a function of the position z by the propagation equation

$$\frac{\partial S_{\parallel,\perp}(z)}{\partial z} = -\alpha(\omega_s)S_{\parallel,\perp}(z) + g_{\parallel,\perp}A_{\text{eff}}^{-1}P_0(L)S_{\parallel,\perp}(z) \times \exp[-\alpha(\omega_p)(L-z)]. \quad (1)$$

Here P_0 and S_0 denote, respectively, power in the pump and probe (Stokes-shifted) light waves, both of which are assumed to propagate along the principal axes of the polarization-maintaining fiber, i.e., without any change in polarization state. The subscripts \parallel and \perp denote, respectively, parallel and perpendicular polarizations of the probe with respect to the pump beam. The Raman gain coefficients, $g_{\parallel,\perp}$, which are functions of the Raman shift $\omega_p - \omega_s$, have units of meters per watt. A_{eff} denotes the effective area of the optical modes within the fiber, as defined in Ref. 7. The effective Raman gain coefficients for

the fiber, which have units of inverse watts per meter, are then given by $g_{\parallel,\perp}A_{\text{eff}}^{-1}$. The linear loss for propagation in the fiber, which includes both absorption and scattering, is described by the frequency-dependent extinction coefficient $\alpha(\omega)$. The relative behavior for the Raman gain in the two polarization configurations is characterized by the depolarization ratio

$$D = g_{\perp}/g_{\parallel}. \quad (2)$$

The general solution of Eq. (1) is given by

$$S_{0\parallel,\perp}(L) = S_{0\parallel,\perp}(0) \exp \left\{ -\alpha(\omega_s)L + g_{\parallel,\perp}A_{\text{eff}}^{-1}P_0(L) \frac{1 - \exp[-\alpha(\omega_p)L]}{\alpha(\omega_p)} \right\}. \quad (3)$$

In the limit of a sufficiently short optical fiber, the linear attenuation of the pump beam will be slight [$\alpha(\omega_p)L \ll 1$], and the Raman gain experienced by the probe will be weak [$g_{\parallel,\perp}A_{\text{eff}}^{-1}P_0(L) \ll 1$]. We can then rewrite Eq. (3) in the following form:

$$S_{0\parallel,\perp}(L) = [1 + g_{\parallel,\perp}A_{\text{eff}}^{-1}P_0(L) - \alpha(\omega_s)L]S_{0\parallel,\perp}(0). \quad (4)$$

This equation underlies the interpretation of our Raman gain measurement for a short optical fiber.

In an experiment, one measures the change in the power that the probe beam experiences in propagating through the fiber in the presence of the Raman pump beam. From the practical standpoint, it may be difficult to differentiate between the two terms in Eq. (4) contributing to this change, the Raman gain and fiber loss terms. The Raman gain term can be isolated by one's modulating the powers of both the pump and the probe beams, each at a distinct frequency. The Raman interaction in Eq. (4) acts to couple the pump and probe powers and produces a modulation in the probe beam power at the sum and difference frequencies. For the strength of the sum-frequency response, we have

$$S_{0\parallel,\perp}(L, f_p + f_s) = \frac{1}{2}g_{\parallel,\perp}A_{\text{eff}}^{-1}LP_0(0)S_{0\parallel,\perp}(0), \quad (5)$$

where f_p and f_s denote, respectively, the modulation frequencies of the pump and probe beams. In this relation, a modulation index of 1 is assumed; for other cases, the pump and probe powers are to be multiplied by their respective modulation indices. This double-modulation scheme clearly eliminates the influence of the linear absorption of the probe beam, as represented by the last term in Eq. (4). In contrast to a scheme in which we simply modulate the pump power and detect the induced change in the probe beam, however, the double-modulation technique has the advantage of discriminating against the unintentional detection of Raman pump radiation. Since the induced modulation in the probe beam will be slight in a short fiber, the influence of back-scattering of the Raman pump radiation in the fiber (particularly for small Raman frequency shifts to which spectral discrimination is difficult to apply) can be significant and can impede correct measurement of the Raman gain.

B. Analysis of Raman Gain for Arbitrary Polarization States

Up to this point, we have treated only linear polarization states, either parallel or perpendicular to one another, for the pump and probe beams in the Raman interaction. We now consider the generalization for arbitrary polarization states. We show that we can describe the gain for arbitrary pump and probe polarization states by using only the two Raman gain coefficients, g_{\parallel} and g_{\perp} , introduced above, with appropriate weightings depending on the precise polarization configuration involved.

For this analysis, we introduce the Raman gain tensor g_{ijkl} . This quantity describes the coupling between the Raman pump electric field and the probe beam at the Stokes frequency for an arbitrary relative polarization of the two beams. The latter two spatial indices correspond to the field of the Raman pump beam, the second index corresponds to the electric field of the Stokes wave, and the first index characterizes the direction in which the Raman gain is experienced. The perpendicular and parallel Raman gain coefficients introduced above thus correspond to $g_{\perp} \equiv g_{xxyy}$ and $g_{\parallel} \equiv g_{xxxx}$.

We may simplify the form of the full Raman gain tensor g_{ijkl} by consideration of symmetry properties. One symmetry relation is provided by the isotropic nature of the material composing the optical fiber:

$$g_{\parallel} = g_{\perp} + g_{xyxy} + g_{xyyx}. \quad (6)$$

A further relation has been derived in Ref. 8 within the approximation that the Raman gain depends only on the Raman shift, $\omega_p - \omega_s$, rather than on either frequency separately. Within the usual nonresonant regime, this is a suitable assumption. Noting that the gain is proportional to the imaginary part of the susceptibility,³ we can write the relation derived in Ref. 8 as

$$g_{\perp} = g_{xyxy}. \quad (7)$$

Combining Eqs. (6) and (7), we then obtain for the remaining tensor element:

$$g_{xyyx} = g_{\parallel} - 2g_{\perp}. \quad (8)$$

We thus see that the complete gain tensor can be expressed, within the given approximation, simply in terms of the $xxxx$ and $xxyy$ tensor elements or, equivalently, in terms of the parallel and perpendicular Raman gain coefficients $g_{\parallel, \perp}$.

Using these relations for the different elements of g_{ijkl} , we can derive by the procedure described in Ref. 9 a generalized relationship for propagation of the probe beams within an optical fiber:

$$\begin{aligned} \frac{\partial S_0(z)}{\partial z} = & -\alpha(\omega_s)S_0(z) \\ & + \frac{1}{2}(g_{\parallel} + g_{\perp})A_{\text{eff}}^{-1}S_0(z)P_0(z) \\ & + \frac{1}{2}(g_{\parallel} - g_{\perp})A_{\text{eff}}^{-1}[S_1(z)P_1(z) + S_2(z)P_2(z)] \\ & + \frac{1}{2}(g_{\parallel} - 3g_{\perp})A_{\text{eff}}^{-1}S_3(z)P_3(z). \end{aligned} \quad (9)$$

Here S_i and P_i (for $i=0,1,2,3$) denote, respectively, the components of the Stokes vector for the probe and Raman pump fields. As above and in conformity with the convention for the Stokes vector, the subscript 0 denotes the total power of the corresponding light wave. In Eq. (9) we do not explicitly describe the propagation of the pump and probe fields along the fiber but rather the evolution of the specified power. Also note that one can write an analogous equation for the evolution of the pump power by interchanging the roles of the pump and probe beams. Equation (9) reduces to Eq. (1) given above for the case of linearly polarized pump and probe beams on substitution of the exponentially decaying form of the (undepleted) pump beam. We summarize in Table 1 the spatially local Raman gain experienced by the probe for some special cases of pump and probe polarizations. These relations follow directly from Eq. (9) by using the Stokes vectors corresponding to the relevant polarization states.

Of particular relevance for our experimental study is the behavior that occurs for a linearly polarized Raman pump beam interacting with a probe beam of arbitrary polarization. From Eq. (9) we find that the probe beam will experience a Raman gain given by

$$\frac{1}{2}(g_{\parallel} + g_{\perp}) + \frac{1}{2}(g_{\parallel} - g_{\perp})m, \quad (10)$$

where the parameter $m \equiv S_1(z)P_1(z)/S_0(z)P_0(z)$ is determined by the relevant Stokes vectors and can assume values between -1 and 1 . This expression can readily be seen to revert to the expected relations for linearly polarized probe beams lying parallel and perpendicular to the pump beam.

In our experiment, a linearly polarized Raman pump beam is launched along one of the principal axes of a polarization-maintaining fiber. This beam will maintain its polarization state as it propagates (neglecting the influence of pump depletion through the Raman interaction). For experimental reasons, the initial polarization state of the probe beam, though readily adjustable, can-

Table 1. Local Raman Gain Properties

Pump ^a	Probe ^a	Gain
Linear	Circular	$\frac{1}{2}(g_{\parallel} + g_{\perp})$
Circular left handed	Circular left handed	$g_{\parallel} - g_{\perp}$
	Circular right handed	$2g_{\perp}$
Circular right handed	Circular right handed	$g_{\parallel} - g_{\perp}$

^aPump and probe polarizations are interchangeable.

not be assumed to lie along a principal axis. The birefringence of the fiber will thus generally cause the probe polarization to evolve as the wave propagates along the fiber. Although the local Raman gain is given by expression (10), the net Raman gain experienced by the probe in propagating through the fiber must be found by integration of expression (10) over the length of the fiber. From consideration of Table 1 we see that the extreme values of the local Raman gain—and, by extension, of the integrated Raman gain—correspond to the parallel and perpendicular values of the Raman gain coefficients, $g_{\parallel, \perp}$. These extrema are realized when the probe beam is either parallel or perpendicular to the pump beam. In these configurations both the pump and the probe beams propagate along principal axes of the fiber, so no evolution of the polarization state needs to be considered. Thus, the expression for the local gain carries over the measured experimental case if the probe polarization is scanned over all possible states. This observation is the basis of our experimental determination of the tensor components of the Raman gain.

3. EXPERIMENTAL SETUP

The experimental arrangement for measurement of the tensor Raman gain in a polarization-maintaining optical fiber is shown schematically in Fig. 1. The source for the Raman pump radiation at wavelength λ_p was a fiber-Bragg-grating-stabilized semiconductor laser. This laser, JDSU 3400 series,¹⁰ was operated at a wavelength of $\lambda_p = 1459$ nm and a power of 125.8 ± 0.1 mW at the fiber under test. (Note that all tolerances and error bars are given at the first standard deviation.) An isolator with non-polarization-maintaining fiber pigtailed was positioned after the pump to prevent its destabilization by backreflection and introduction of the counterpropagating probe radiation. We used a three-loop polarization controller fol-

lowed by a polarization beam combiner to launch the light along a principal axis of the polarization-maintaining fiber under test. After passing through the fiber, the pump radiation was rejected by the circulator.

The probe light, at wavelength λ_s , was generated by a Photonics Tunics Plus¹⁰ tunable external-cavity laser. This source was operated at a power of 0.47 ± 0.01 mW at the fiber under test in the experiment. The source could be readily tuned over wavelengths longer than the pump wavelength λ_p to provide the desired Raman frequency shift. Its spectral width was approximately 10 MHz. The output of the probe laser passed through a motorized three-loop polarization controller, which served to vary its polarization state over time. The probe beam then passed through the circulator into the fiber under test, where it propagated in the opposite direction of the pump beam. The amplified probe light was extracted through the 10% arm of the 90/10 splitter and was monitored by an In-GaAs photodiode.

The silica-based optical fiber under test, type SM.13-P-7/125UV/UV-400, was supplied by Fujikura.¹⁰ On the basis of the Raman spectra that we acquired (using the spontaneous Raman-scattering approach described below) and data in Refs. 11 and 12, we estimate the fiber's concentration of GeO_2 at 2.4 mol.%. The fiber maintained the polarization state using stress-inflicted birefringence (PANDA type); it exhibited a polarization cross talk of -33.8 dB, a group beat length of 3.2 mm, and a loss of 0.27 dB/km at a wavelength of $1.3 \mu\text{m}$. In our measurements a 10 m length of the fiber was used.

In our double-modulation scheme, the pump laser power was modulated electrically through the laser controller at a frequency of $1.0 \text{ kHz} \pm 25 \text{ mHz}$. This relatively low modulation frequency was constrained by the properties of the laser controller. The probe laser was also electrically modulated but at a frequency of $8.7 \text{ MHz} \pm 100 \text{ Hz}$. The electrical output of the photodiode

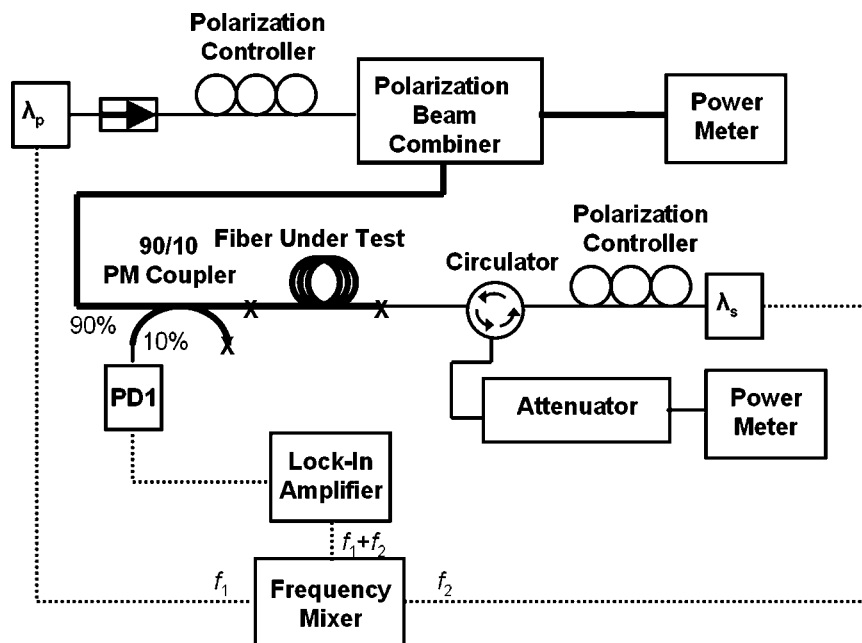


Fig. 1. Schematic of the apparatus for the Raman gain measurement. Thick solid lines, the polarization-maintaining fiber; thin solid lines, the single-mode fiber. Electrical connections are shown by dashed lines. PD, photodiode; PM, polarization maintaining.

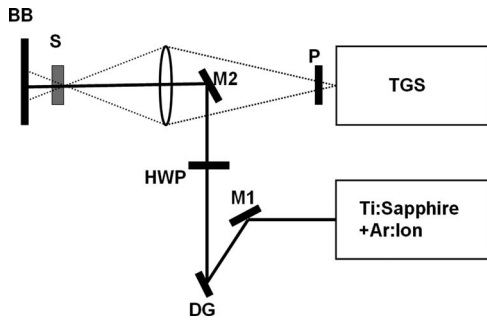


Fig. 2. Apparatus for spontaneous Raman scattering in a bulk sample, as described in the text.

detecting the probe beam was processed with a lock-in amplifier. The reference frequency for the lock-in amplifier was the sum of the probe and pump modulation frequencies. The double-modulation technique permitted measuring an increase in power of 1 part per 10^9 .

To acquire data on the polarization-dependent Raman gain, we recorded the gain of the probe beam from the lock-in amplifier while scanning the probe polarization over full Poincaré sphere of polarization states. The maxima and minima correspond, as discussed above, to the parallel and perpendicular Raman gain coefficients. To obtain frequency-dependent data, we repeated the polarization scan for many different choices of probe wavelength over a range of Raman frequency shifts from below 1 to above 15 THz.

Figure 2 shows the experimental setup for acquiring the spontaneous Raman-scattering spectra from a bulk sample. The scheme constitutes a standard arrangement for performing Raman spectroscopy by using excitation by a single-mode longitudinal mode of a pump laser and detection by a triple-grating spectrometer. For the laser source, we used a Ti:sapphire ring laser (Coherent 899 ring laser)¹⁰ pumped by an argon-ion laser (Coherent Innova Sabre with multiline visible head).¹⁰ This provided a tunable source with a power of $1\text{ W} \pm 10\text{ mW}$. The light beam from the Ti:sapphire laser was directed by mirror M1 onto diffraction grating DG in order to filter out any power from longitudinal satellite modes of the laser. The light passed through a half-wave plate HWP for polarization control and was directed by mirror M2 (of diameter $10 \pm 0.1\text{ mm}$) onto sample S. Behind the sample, a beam block BB served to absorb the transmitted pump radiation. The spontaneous Raman emission produced by the sample in the backscattered direction was collected by a lens L (of diameter $76 \pm 0.1\text{ mm}$), passed through a polarizer P to attenuate the horizontal polarization by $20 \pm 1\text{ dB}$, and was focused into a triple-grating spectrometer TGS (Dilor XY800).¹⁰ The solid angle of collection was $0.063\text{ sr} \pm 1\%$. The output of the spectrometer was detected by a CCD array. The polarization extinction ratio of the half-wave plate and analyzer was measured to be $15 \pm 1\text{ dB}$. The TGS provided another $10 \pm 1\text{ dB}$ of polarization-dependent loss. The total uncertainty in the polarization extinction ratio, which includes the influence of laser intensity fluctuations, is 4.8%. The sample used in these measurements was a bulk high-purity fused-silica specimen.

4. RESULTS AND DISCUSSION

The experimental Raman gain coefficients for the fiber measurement are plotted in Fig. 3 as a function of the Raman frequency shift $\omega_p - \omega_s$. The data for Raman frequency shifts were constrained at low frequencies by the weakness of the Raman signal. The general form obtained for the frequency dependence of the parallel gain g_0 agrees well with reports in the literature.⁷ We have not attempted to make an absolute calibration of the gain coefficient and show only the relative Raman gain.

To examine the behavior of the parallel and perpendicular Raman gains more precisely, we plot in Fig. 4 the depolarization ratio $D = g_{\perp} / g_{\parallel}$. The data show a depolarization ratio that drops from approximately 0.3 to a value of less than 0.05 near the 13 THz peak in the Raman gain. The general trend of a decreasing depolarization ratio for increasing Raman frequency shifts has been reported elsewhere.⁷ The behavior for small Raman frequency shifts, however, differs from previous determinations based on direct fiber measurements of the polarized Raman gain. In Ref. 5, a low-frequency value of $D = 0.45 \pm 0.05$ was reported. The results of Ref. 6 yield an even larger ratio that increases with decreasing wave-

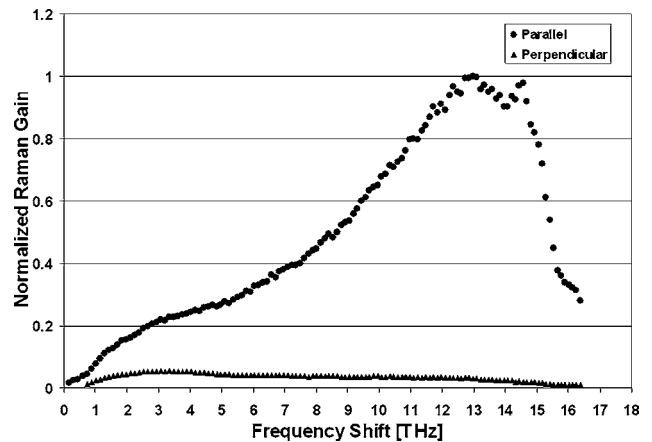


Fig. 3. Experimental data for the polarized Raman gain in an optical fiber as a function of the Raman frequency shift.

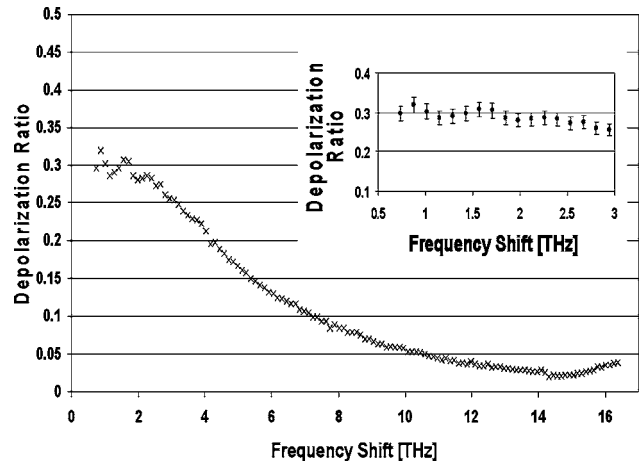


Fig. 4. Experimental depolarization ratio D of the Raman gain. The inset shows the depolarization ratio for small Raman frequency shifts.

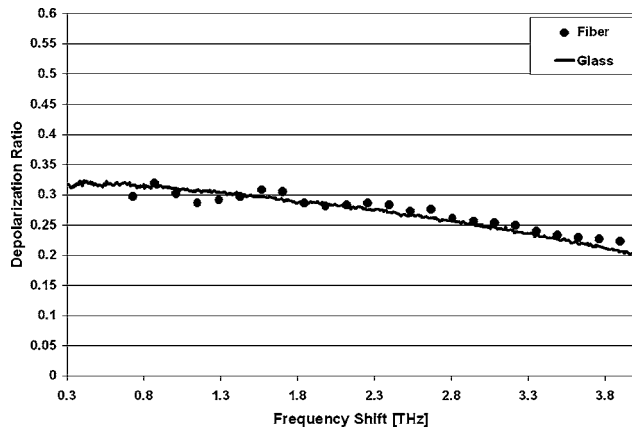


Fig. 5. Comparison of the experimental depolarization ratio measured by the Raman gain technique in an optical fiber (points) and spontaneous Raman scattering in a bulk sample (curve). The uncertainty in the spontaneous Raman measurement is $\pm 4.8\%$.

length. Indeed, the fit of the experimental results in Ref. 6 implies a limiting behavior for a vanishing frequency shift of $D=1$. Our results, presented in Fig. 4, yield a depolarization ratio of $D=0.30\pm 0.05$ in the low-frequency regime, without any pronounced increase as the frequency shift approaches 0.

Spontaneous Raman-scattering measurements can also provide direct information on the depolarization ratio by a comparison of the strength of the Raman scattering for orthogonal polarizations. To address the discrepancy in data obtained in the current and prior fiber measurements of the Raman gain for small Raman frequency shifts, we performed a complementary set of measurements using spontaneous Raman scattering. The results for the frequency-dependent depolarization ratio D are displayed in Fig. 5. The data represent the mean for excitation at three distinct pump wavelengths (780.0, 773.8, and 810.5 nm). In Fig. 5 we compare these results with the data obtained from the Raman gain measurement in the fiber (Fig. 4) and find excellent agreement. Note that the present measurements of D are also consistent with other data in the literature based on spontaneous Raman scattering from fused silica.^{1,7}

The comparison of the measurements of the depolarization ratio using the Raman gain measurements in a fiber and spontaneous Raman scattering in a bulk sample is informative. The close agreement indicates that the Raman gain characteristics are not strongly influenced by the choice of frequency of the Raman pump beam: in the spontaneous measurement, a wavelength near 800 nm was used, whereas the Raman gain measurements used a wavelength near 1500 nm. This behavior is not unexpected, since both frequencies lie significantly below that of the optical transitions in silica. Also note that the details of the stoichiometry and processing of the two samples also had a significant effect on the Raman gain characteristics: the sample for the spontaneous Raman measurements was a bulk piece of fused silica, and the material for the Raman gain measurements was a GeO₂-doped optical fiber. This behavior is also understandable, since the composition of the optical fiber is still dominated by its SiO₂ component. Of course, the detailed

spectroscopic features of the Raman gain will reflect these subtle differences, particularly through the presence of distinctive vibrational modes associated with the dopants.

5. CONCLUSION

In this paper we have presented a sensitive technique for measuring the components of the Raman gain tensor in silica optical fibers. The method provides several advantages over previous techniques for characterizing the Raman gain in optical fibers: (1) the double-modulation technique allows a short piece of fiber to be characterized, leading toward analysis of non-polarization-maintaining fibers; (2) the method uses off-the-shelf fiber components in a simple experimental arrangement; and (3) the only polarization critical path is that of the pump, thus minimizing the complications of delicate polarization alignment.

Using this experimental approach, we determined the Raman gain and depolarization ratio for frequency shifts from below 1 to above 15 THz. The results for the depolarization ratio were confirmed by a spontaneous Raman-scattering measurement in a bulk sample. This comparison validated the method even in the difficult regime of small Raman frequency shifts, where a depolarization ratio of $D=0.32\pm 0.03$ was obtained.

ACKNOWLEDGMENTS

I. Mandelbaum thanks Nicholas King for useful discussions and a National Institute of Standards and Technology–National Research Council postdoctoral fellowship for partial financial support. Work at Columbia University was supported by a grant from the Infotonics Technology Center.

I. Mandelbaum, the corresponding author, can be reached by e-mail at idan.mandelbaum@nist.gov.

REFERENCES AND NOTES

1. G. Winterling, "Very-low-frequency Raman scattering in vitreous silica," *Phys. Rev. B* **12**, 2432–2440 (1975).
2. D. M. Krol and J. G. van Lierop, "The densification of monolithic gels," *J. Non-Cryst. Solids* **63**, 131–144 (1984).
3. G. P. Agrawal, *Nonlinear Fiber Optics*, 3rd ed. (Academic, 2001).
4. A. Saissy, "Spontaneous Raman scattering and polarization mode coupling in polarization-maintaining optical fibers," *J. Lightwave Technol.* **LT-5**, 1045–1049 (1987).
5. D. J. Dougherty, F. X. Kartner, H. A. Haus, and E. P. Ippen, "Measurement of the Raman gain spectrum of optical fibers," *Opt. Lett.* **20**, 31–33 (1995).
6. X. Li, P. L. Voss, J. Chen, K. F. Lee, and P. Kumar, "Measurement of co- and cross-polarized Raman spectra in silica fiber for small detunings," *Opt. Express* **13**, 2236–2244 (2005).
7. R. H. Stolen, "Issues in Raman gain measurements," in *Technical Digest Symposium on Optical Fiber Measurements* (National Institute of Standards and Technology, 2000), pp. 139–142.
8. S. V. Chernikov and P. V. Mamyshev, "Effect of polarization on Raman scattering in optical fibers," *Sov. Lightwave Commun.* **1**, 301–312 (1991).
9. Y. P. Svirko and N. I. Zheludev, "Propagation of partially polarized light," *Phys. Rev. A* **50**, 709–713 (1994).
10. Disclaimer: Certain commercial equipment, software, instruments, or materials are identified in this paper to

foster understanding and does not imply recommendation or endorsement by National Institute of Standards and Technology, nor does it imply that the material or equipment identified are necessarily the best available for that purpose.

11. S. T. Davey, D. L. Williams, B. J. Ainslie, W. J. M. Rothwell, and B. Wakefield, "Optical gain spectrum of GeO₂-SiO₂ Raman fibre amplifiers," *IEE Proc.-J: Optoelectron.* **136**, 301-306 (1989).
12. Y. Kang, "Calculations and measurements of Raman gain coefficients of different fiber types," M.S. thesis (Virginia Institute of Technology, Blacksburg, Va., 2002).